

Probing the hadron mass spectrum in dense two-color QCD with the linear sigma model

Daiki Suenaga^{1,2,*}, Kotaro Murakami^{3,4,†}, Etsuko Itou^{2,4,5,‡} and Kei Iida^{6,§}

¹*Strangeness Nuclear Physics Laboratory, RIKEN Nishina Center, Wako 351-0198, Japan*

²*Research Center for Nuclear Physics, Osaka University, Ibaraki 567-0048, Japan*

³*Yukawa Institute for Theoretical Physics, Kyoto University, Kyoto 606-8502, Japan*

⁴*Interdisciplinary Theoretical and Mathematical Sciences Program (iTHEMS), RIKEN, Wako 351-0198, Japan*

⁵*Department of Physics, and Research and Education Center for Natural Sciences, Keio University, 4-1-1 Hiyoshi, Yokohama, Kanagawa 223-8521, Japan*

⁶*Department of Mathematics and Physics, Kochi University, 2-5-1 Akebono-cho, Kochi 780-8520, Japan*



(Received 10 November 2022; accepted 3 February 2023; published 1 March 2023)

We investigate modifications of hadron masses at finite quark chemical potential in two-flavor and two-color QCD, data of which are available from lattice simulations, within a linear sigma model based on approximate Pauli-Gursey $SU(4)$ symmetry. The model describes not only ground-state scalar diquarks and pseudoscalar mesons but also the excited pseudoscalar diquarks and scalar mesons; each ground-state diquark (meson) has the corresponding excited diquark (hadron) with opposite parity as a chiral partner. Effects of chiral symmetry breaking and diquark condensates are incorporated by a mean-field treatment. We show that various mixings among the hadrons, which are triggered by the breakdown of baryon number conservation in the superfluid phase, lead to a rich hadron mass spectrum. We discuss the influence of $U(1)_A$ anomaly on the density dependence of the mass spectrum and also manifestations of the chiral partner structures as the density increases in the superfluid phase. The predicted hadron masses are expected to provide future lattice simulations with useful information on such symmetry properties in dense two-color QCD.

DOI: [10.1103/PhysRevD.107.054001](https://doi.org/10.1103/PhysRevD.107.054001)

I. INTRODUCTION

Toward understanding quantum chromodynamics (QCD) at finite quark chemical potential μ_q , two-color QCD (QC₂D) with an even number of quark flavors is useful since in such a QCD-like theory *lattice QCD* simulations work even at finite μ_q without suffering from the so-called *sign problem* [1,2]. Based on this advantage, so far many efforts from lattice QCD simulations at finite μ_q in QC₂D have been devoted to understanding of, e.g., modifications of hadron masses, gluon propagators, phase diagram of QC₂D, electromagnetic transport coefficients, and so on [3–26]. Therefore, lattice simulations in QC₂D at

finite μ_q serve as a *numerical experiment* for future investigation of dense QCD.

Although lattice simulations are powerful, they only provide us with numerical information. In this regard, examinations of the simulation results based on effective models give us deeper insights into dense QCD. Motivated by this fact, hadron mass modifications and phase structures at finite μ_q were theoretically investigated within chiral perturbation theory [27–31], hidden local symmetry (HLS) [32], Nambu-Jona-Lasinio (NJL)-type model [33–44], and quark-meson coupling model with the functional method [45–47]. Delineation of gluon propagators and transport coefficients in dense QC₂D was also attempted by using the Dyson-Schwinger equation [48] as well as by combining a massive gluon model with quasiparticle description of quarks [49–51]. In addition to those field-theoretical approaches, which are broadly employed, recently a unified picture that connects the smooth transition from hadronic matter to quark matter with the quark model has been developed [52,53]. From these studies, it is expected that a deeper understanding of dense QC₂D properties, most of which are commonly shared by three-color QCD, is achieved [54].

*daiki.suenaga@riken.jp

†kotaro.murakami@yukawa.kyoto-u.ac.jp

‡itou@yukawa.kyoto-u.ac.jp

§iida@kochi-u.ac.jp

Published by the American Physical Society under the terms of the [Creative Commons Attribution 4.0 International license](https://creativecommons.org/licenses/by/4.0/). Further distribution of this work must maintain attribution to the author(s) and the published article's title, journal citation, and DOI. Funded by SCOAP³.

In QC₂D, diquarks made of two quarks form a color singlet and hence can be regarded as baryons. Accordingly, baryonic matter is formed as a many-body system of diquarks obeying the Bose-Einstein statistics. As a result, when the baryon chemical potential or, equivalently, the quark chemical potential μ_q exceeds a certain critical value, the Bose-Einstein condensate (BEC) phase of diquarks emerges at sufficiently low temperature [27,28]. The phase is often called the *diquark condensed phase* or the *baryon superfluid phase* since the baryon number conservation is violated here. In contrast, the normal phase with no BECs, which is continuously connected to the vacuum, i.e., the system with vanishing temperature and chemical potential, is simply referred to as the *hadronic phase*. In this phase, all thermodynamic quantities are independent of μ_q , which is known as the *Silver Blaze property*.

Emergence of the baryon superfluidity is manifestly reflected by hadron mass spectrum. For instance, the baryon number violation in the superfluid phase causes mixings among mesons and diquarks having identical quantum numbers [33]. The appearance of the Nambu-Goldstone (NG) bosons in association with the breakdown of $U(1)_B$ baryon number symmetry is another striking consequence [27,28]. For this reason, lattice simulations that reveal modifications of hadron masses in the baryon superfluid phase as well as in the hadronic phase were performed by several groups [3,4,6,9,19,55]. In particular, in Ref. [55] the simulation was extended in such a way as to include not only the ground-state hadrons but also the orbitally excited ones having opposite parities.

Motivated by the above progress in lattice studies, in the present study, we theoretically investigate hadron mass modifications in both the hadronic and baryon superfluid phases at zero temperature by utilizing a linear sigma model [56]. Since the linear sigma model is based on the linear representation of quarks, the model has two noteworthy advantages from the symmetry point of view: (i) The model can describe both the ground-state hadrons and excited ones in a unified way, which allows us to identify the *chiral partners*. (ii) The model can incorporate changes of the ground-state configurations associated with in-medium chiral-symmetry restoration in a broad range of μ_q at mean-field level [57].¹ In particular, we concentrate on spin-zero hadrons in this exploratory work where inputs are provided by the recent lattice results [55]. Then, we demonstrate how symmetry properties related to chiral symmetry and $U(1)_A$ axial anomaly in dense QC₂D are extracted by the mass spectrum. Moreover, we present

predictions of novel hadron mass modifications, which might provide useful information on the symmetry insights of dense QC₂D for future lattice simulations.

This article is organized as follows. In Sec. II, general properties of QC₂D are briefly explained, and accordingly the linear sigma model to investigate hadron mass modifications at finite μ_q is introduced. In Sec. III, input information from recent lattice simulations is presented, and we therefrom examine the μ_q dependence of mean fields to delineate the emergence of the baryon superfluid phase. In Sec. IV the resultant hadron mass spectra at finite μ_q are demonstrated by focusing on effects of $U(1)_A$ anomaly, and also discussions on the chiral partner structures are provided. In Sec. V we conclude the present work.

II. MODEL

In this section, we construct our linear sigma model from symmetry arguments.

A. General properties of QC₂D

Within the linear sigma model, hadron states are provided by the linear representation of quark bilinears sharing the same symmetry properties, which in turn determine the structure of hadron interactions. In QC₂D with two flavors ($N_f = 2$), the flavor symmetry is characterized by the Pauli-Gursey $SU(4)$ symmetry [27,28,69,70] rather than $SU(2)_L \times SU(2)_R \times U(1)_B$. In this subsection, before presenting our linear sigma model we briefly review emergence of the Pauli-Gursey $SU(4)$ symmetry by turning back to the fundamental QC₂D Lagrangian.

The QC₂D Lagrangian for massless two quarks ($N_f = 2$) is of the form

$$\mathcal{L}_{\text{QD}} = \bar{\psi} i \not{D} \psi, \quad (1)$$

where $\psi = (u, d)^T$ is the quark doublet and $D_\mu \psi = \partial_\mu \psi + ig_c A_\mu^a T_c^a \psi$ is the covariant derivative describing interactions between the quarks and gluons, with $T_c^a = \tau_c^a/2$ being the $SU(2)_c$ generator (τ_c^a is the Pauli matrix in color space). Introducing the Weyl representation for the Dirac matrices for convenience, one can express the Lagrangian (1) in terms of left-handed and right-handed quarks as

$$\begin{aligned} \mathcal{L}_{\text{QC}_2\text{D}} = & \psi_R^\dagger i \partial_\mu \sigma^\mu \psi_R - g_c \psi_R^\dagger A_\mu^a T_c^a \sigma^\mu \psi_R \\ & + \psi_L^\dagger i \partial_\mu \bar{\sigma}^\mu \psi_L - g_c \psi_L^\dagger A_\mu^a T_c^a \bar{\sigma}^\mu \psi_L. \end{aligned} \quad (2)$$

In this Lagrangian, we have used $u = (u_R, u_L)^T$ and $d = (d_R, d_L)^T$ in the Weyl representation, and defined two component matrices $\sigma^\mu = (\mathbf{1}, \sigma^i)$ and $\bar{\sigma}^\mu = (\mathbf{1}, -\sigma^i)$ in spinor space with the Pauli matrix σ^i . Here, we utilize the pseudoreality of the Pauli matrix to obtain the relations

$$T_c^a = -\tau_c^2 (T_c^a)^T \tau_c^2, \quad \sigma^i = -\sigma^2 (\sigma^i)^T \sigma^2, \quad (3)$$

¹Investigation of modifications of light hadron masses from the aspect of chiral restoration at finite density through the linear sigma model of three-color QCD have been done widely by several methods [58–67] such as functional methods. The model has also been applied to QCD with an isospin chemical potential [68].

and accordingly introduce “conjugate quarks”:

$$\tilde{\psi}_R \equiv \sigma^2 \tau_c^2 \psi_R^*, \quad \tilde{\psi}_L \equiv \sigma^2 \tau_c^2 \psi_L^*. \quad (4)$$

Then, the Lagrangian (2) can be expressed in a unified form as

$$\mathcal{L}_{\text{QC}_2\text{D}} = \Psi^\dagger i \partial_\mu \sigma^\mu \Psi - g_c \Psi^\dagger A_\mu^a T_c^a \sigma^\mu \Psi, \quad (5)$$

when we introduce the four-component column vector as

$$\Psi \equiv \begin{pmatrix} \psi_R \\ d_R \\ \tilde{\psi}_L \\ \tilde{d}_L \end{pmatrix}. \quad (6)$$

The Lagrangian (5) is obviously invariant under $SU(4)$ transformation of Ψ :

$$\Psi \rightarrow g \Psi, \quad (7)$$

with $g \in SU(4)$,² rather than $SU(2)_L \times SU(2)_R \times U(1)_B$ chiral transformation. This extended symmetry is sometimes referred to as the Pauli-Gursey symmetry. As can be seen from Eq. (6), the Pauli-Gursey symmetry is realized by treating ψ and the conjugate quarks $\tilde{\psi}$ as one quartet.

The baryon number symmetry, i.e., quark number symmetry, is embedded in the $SU(4)$ symmetry. In fact, from Eq. (6) the quark number transformation reads

$$\Psi \rightarrow e^{-i\theta_q J} \Psi \quad \text{with} \quad J \equiv \begin{pmatrix} \mathbf{1} & 0 \\ 0 & -\mathbf{1} \end{pmatrix}. \quad (8)$$

On the other hand, the $U(1)_A$ transformation is generated by a unit matrix as

$$\Psi \rightarrow e^{-i\theta_A I} \Psi \quad \text{with} \quad I \equiv \begin{pmatrix} \mathbf{1} & 0 \\ 0 & \mathbf{1} \end{pmatrix}. \quad (9)$$

One of the most characteristic properties of QC_2D is the symmetry-breaking pattern triggered by a chiral condensate $\langle \bar{\psi} \psi \rangle$. Using Eq. (6) one can check

$$\bar{\psi} \psi = -\frac{1}{2} (\Psi^T \sigma^2 \tau_c^2 E \Psi + \Psi^\dagger \sigma^2 \tau_c^2 E^T \Psi^*), \quad (10)$$

with

$$E \equiv \begin{pmatrix} 0 & \mathbf{1} \\ -\mathbf{1} & 0 \end{pmatrix} \quad (11)$$

²We consider only $SU(4)$ symmetry but not $U(4)$ one, since the $U(1)_A$ axial symmetry is explicitly broken due to the anomaly.

the 4×4 symplectic matrix. Equation (10) implies that the chiral condensate $\langle \bar{\psi} \psi \rangle$ is invariant under transformations satisfying

$$h^T E h = E, \quad (12)$$

where h is an element of $Sp(4)$ belonging to a subgroup of the original $SU(4)$. In other words, the symmetry-breaking pattern triggered by the chiral condensate is $SU(4) \rightarrow Sp(4)$ [27,28].

Based on the general properties of QC_2D presented in this subsection, we introduce hadron fields from the quark bilinears in Sec. II B and construct the linear sigma model in such a way as to respect $SU(4)$ symmetry in Sec. II C.

B. Flavor matrix Σ

The advantage of employing the linear sigma model of QCD is that we can simultaneously investigate the ground-state hadrons and their chiral partners having opposite parities, i.e., the P -wave excited states in the quark-model sense, on an equal footing [56]. Such an advantage is explicitly implemented by introducing a flavor matrix Σ containing the hadrons defined through a quark bilinear field in the linear representation. Here, we introduce the corresponding 4×4 Σ matrix in QC_2D and present its properties.

As shown in Sec. II A, QC_2D has the Pauli-Gursey $SU(4)$ symmetry when the quarks are massless, and accordingly any hadronic theory has to respect the symmetry as well. Hence, one useful definition of Σ in terms of the quark bilinear field may be³

$$\Sigma_{ij} \sim \Psi_j^T \sigma^2 \tau_c^2 \Psi_i. \quad (13)$$

This Σ is a flavor 4×4 matrix labeled by i and j , where the summations over spinor and color indices are implicitly done. The flavor matrix Σ is antisymmetric as $\Sigma = -\Sigma^T$ due to the Grassman nature of Ψ . One can see that Σ transforms homogeneously under the $SU(4)$ as

$$\Sigma \rightarrow g \Sigma g^T, \quad (14)$$

from the linear transformation law of the quartet in Eqs. (6) and (7). More explicitly, the Σ in Eq. (13) takes the form of

³Here, the symbol “ \sim ” denotes the correspondence between the composite state in the linear sigma model and the quark bilinear in QC_2D .

$\Sigma \sim$

$$\begin{pmatrix} 0 & d_R^T \sigma^2 \tau_c^2 u_R & u_L^\dagger u_R & d_L^\dagger u_R \\ -d_R^T \sigma^2 \tau_c^2 u_R & 0 & u_L^\dagger d_R & d_L^\dagger d_R \\ -u_L^\dagger u_R & -u_L^\dagger d_R & 0 & d_L^\dagger \sigma^2 \tau_c^2 u_L^* \\ -d_L^\dagger u_R & -d_L^\dagger d_R & -d_L^\dagger \sigma^2 \tau_c^2 u_L^* & 0 \end{pmatrix}. \quad (15)$$

Equation (15) implies that mesons and diquark baryons can be treated in a unified way. To see such a structure more clearly, we try to rewrite the matrix (15) in terms of hadronic states. For this reason, we define interpolating fields for the hadrons by

$$\sigma \sim \bar{\psi} \psi = u_L^\dagger u_R + d_L^\dagger d_R + u_R^\dagger u_L + d_R^\dagger d_L, \quad (16)$$

$$\begin{aligned} a_0^+ &\sim \frac{1}{\sqrt{2}} \bar{\psi} \tau_f^- \psi = \sqrt{2} (d_L^\dagger u_R + d_R^\dagger u_L), \\ a_0^- &\sim \frac{1}{\sqrt{2}} \bar{\psi} \tau_f^+ \psi = \sqrt{2} (u_L^\dagger d_R + u_R^\dagger d_L), \\ a_0^0 &\sim \bar{\psi} \tau_f^3 \psi = u_L^\dagger u_R - d_L^\dagger d_R + u_R^\dagger u_L - d_R^\dagger d_L, \end{aligned} \quad (17)$$

$$\eta \sim \bar{\psi} i \gamma_5 \psi = i(u_L^\dagger u_R + d_L^\dagger d_R - u_R^\dagger u_L - d_R^\dagger d_L), \quad (18)$$

$$\begin{aligned} \pi^+ &\sim \frac{1}{\sqrt{2}} \bar{\psi} i \gamma_5 \tau_f^- \psi = \sqrt{2} i (d_L^\dagger u_R - d_R^\dagger u_L), \\ \pi^- &\sim \frac{1}{\sqrt{2}} \bar{\psi} i \gamma_5 \tau_f^+ \psi = \sqrt{2} i (u_L^\dagger d_R - u_R^\dagger d_L), \\ \pi^0 &\sim \bar{\psi} i \gamma_5 \tau_f^3 \psi = i(u_L^\dagger u_R - d_L^\dagger d_R - u_R^\dagger u_L + d_R^\dagger d_L), \end{aligned} \quad (19)$$

$$\begin{aligned} B &\sim -\frac{i}{\sqrt{2}} \psi^T C \gamma_5 \tau_c^2 \tau_f^2 \psi \\ &= -\sqrt{2} i (d_R^T \sigma^2 \tau^2 u_R + d_L^T \sigma^2 \tau^2 u_L), \\ \bar{B} &\sim -\frac{i}{\sqrt{2}} \psi^\dagger C \gamma_5 \tau_c^2 \tau_f^2 \psi^* \\ &= -\sqrt{2} i (d_R^\dagger \sigma^2 \tau^2 u_R^* + d_L^\dagger \sigma^2 \tau^2 u_L^*), \\ B' &\sim -\frac{1}{\sqrt{2}} \psi^T C \tau_c^2 \tau_f^2 \psi \\ &= -\sqrt{2} (d_R^T \sigma^2 \tau^2 u_R - d_L^T \sigma^2 \tau^2 u_L), \\ \bar{B}' &\sim \frac{1}{\sqrt{2}} \psi^\dagger C \tau_c^2 \tau_f^2 \psi^* \\ &= \sqrt{2} (d_R^\dagger \sigma^2 \tau^2 u_R^* - d_L^\dagger \sigma^2 \tau^2 u_L^*), \end{aligned} \quad (20)$$

with $\tau_f^\pm = \tau_f^1 \pm i \tau_f^2$ (τ_f^a is the Pauli matrix in flavor space) and $C = i \gamma^2 \gamma^0$ the charge-conjugation operator. For the mesons defined in Eqs. (16)–(19), we have employed the notations which are ordinarily adopted in three-color QCD, and thus their chiral properties are well known. For the

baryons defined in Eqs. (20) and (21), current structures are largely different from the case of three-color QCD where baryons are composed of three quarks; B and \bar{B} represent diquark and antidiquark baryons, respectively, which are singlet in both spin and isospin and characterized by $J^P = 0^+$, while B' and \bar{B}' are their chiral partners carrying opposite parities. In fact, B (\bar{B}) and B' (\bar{B}') are interchanged under the $SU(2)_A$ axial transformation. In order to manifestly display the properties, we tabulate quantum numbers of the hadrons in Table I.

Using the hadronic states defined in Eqs. (16)–(21), the matrix (15) can be described in terms of the hadrons as

$$\Sigma = \mathcal{N} \begin{pmatrix} 0 & -B' + iB & \frac{\sigma - i\eta + a^0 - i\pi^0}{\sqrt{2}} & a^+ - i\pi^+ \\ B' - iB & 0 & a^- - i\pi^- & \frac{\sigma - i\eta - a^0 + i\pi^0}{\sqrt{2}} \\ -\frac{\sigma - i\eta + a^0 - i\pi^0}{\sqrt{2}} & -a^- + i\pi^- & 0 & -\bar{B}' + i\bar{B} \\ -a^+ + i\pi^+ & -\frac{\sigma - i\eta - a^0 + i\pi^0}{\sqrt{2}} & \bar{B}' - i\bar{B} & 0 \end{pmatrix}. \quad (22)$$

As for the normalization constant \mathcal{N} , we take $\mathcal{N} = 1/2$ for later use.

The matrix (22) implies that when σ is replaced by its mean field σ_0 responsible for the chiral condensate $\langle \bar{\psi} \psi \rangle$, the vacuum expectation value (VEV) of Σ is proportional to the symplectic matrix:

$$\langle \Sigma \rangle_{\text{ch}} \propto E. \quad (23)$$

Thus, from the transformation law in Eq. (14) we see that the VEV $\langle \Sigma \rangle_{\text{ch}}$ is singlet only when g is replaced by h satisfying Eq. (12), which obviously reflects the symmetry-breaking pattern of $SU(4) \rightarrow Sp(4)$ as explained at the end of Sec. II A.

The matrix (22) can be written in a more compact form. In fact, once one defines S^a , P^a , B^i , and B'^i as

TABLE I. Quantum numbers carried by the hadrons defined in Eqs. (16)–(21).

Hadron	J^P	Quark number	Isospin
σ	0^+	0	0
a_0	0^+	0	1
η	0^-	0	0
π	0^-	0	1
B (\bar{B})	0^+	$+2(-2)$	0
B' (\bar{B}')	0^-	$+2(-2)$	0

$$\begin{aligned}
\sigma &= S^0, & a_0^0 &= S^3, & a_0^\pm &= \frac{S^1 \mp iS^2}{\sqrt{2}} \\
\eta &= P^0, & \pi^0 &= P^3, & \pi^\pm &= \frac{P^1 \mp iP^2}{\sqrt{2}}, \\
B &= \frac{B^5 - iB^4}{\sqrt{2}}, & \bar{B} &= \frac{B^5 + iB^4}{\sqrt{2}}, \\
B' &= \frac{B'^5 - iB'^4}{\sqrt{2}}, & \bar{B}' &= \frac{B'^5 + iB'^4}{\sqrt{2}},
\end{aligned} \quad (24)$$

and some generators of $U(4)$ as

$$\begin{aligned}
X^a &= \frac{1}{2\sqrt{2}} \begin{pmatrix} \tau_f^a & 0 \\ 0 & (\tau_f^a)^T \end{pmatrix} \quad (a = 0-3), \\
X^i &= \frac{1}{2\sqrt{2}} \begin{pmatrix} 0 & D_f^i \\ (D_f^i)^\dagger & 0 \end{pmatrix} \quad (i = 4, 5),
\end{aligned} \quad (25)$$

with $\tau_f^0 = \mathbf{1}$, $D_f^4 = \tau_f^2$ and $D_f^5 = i\tau_f^2$, the matrix (22) turns into

$$\Sigma = (S^a - iP^a)X^a E + (B'^i - iB^i)X^i E. \quad (26)$$

The flavor matrix (26) together with its transformation property (14) enables us to construct the linear sigma model in a familiar way but now based on the Pauli-Gursey $SU(4)$ symmetry of QC_2D .

C. Linear sigma model

In this subsection we construct the linear sigma model from the flavor matrix Σ , which allows us to investigate the hadron mass spectrum at finite quark chemical potential.

From the flavor matrix (26) with the transformation property (14), our linear sigma model that approximately preserves the Pauli-Gursey $SU(4)$ symmetry can be obtained as⁴

$$\begin{aligned}
\mathcal{L}_{\text{LSM}} &= \text{tr}[D_\mu \Sigma^\dagger D^\mu \Sigma] - m_0^2 \text{tr}[\Sigma^\dagger \Sigma] - \lambda_1 (\text{tr}[\Sigma^\dagger \Sigma])^2 \\
&\quad - \lambda_2 \text{tr}[(\Sigma^\dagger \Sigma)^2] + \text{tr}[H^\dagger \Sigma + \Sigma^\dagger H] \\
&\quad + c(\det \Sigma + \det \Sigma^\dagger).
\end{aligned} \quad (27)$$

In Eq. (27), we have left the flavor matrices up to the fourth order in Σ (Σ^\dagger) such that the theories are renormalizable as widely done for the three-color version of linear sigma model [71–73]. H is defined by

$$H = h_q E, \quad (28)$$

which describes the explicit breaking of the chiral symmetry or the Pauli-Gursey $SU(4)$ symmetry. Here, h_q is a

⁴Due to $\Sigma^\dagger = -\Sigma^*$, for instance, $\text{tr}[\Sigma^* \Sigma]$ is identical to $-\text{tr}[\Sigma^\dagger \Sigma]$.

constant which captures the effects of the current quark masses.

Besides, the $U(1)_A$ axial transformation for Σ is $\Sigma \rightarrow e^{-i\theta_A I} \Sigma e^{-i\theta_A I}$ as can be understood from Eq. (9), and hence the Kobayashi–Maskawa–’t Hooft (KMT)-type term proportional to c is responsible for the $U(1)_A$ axial anomaly [74–77]. The covariant derivative with respect to $U(1)_B$ symmetry in Eq. (27) is defined by

$$D_\mu \Sigma = \partial_\mu \Sigma - i(\mathcal{V}_\mu \Sigma + \Sigma \mathcal{V}_\mu^T), \quad (29)$$

where the “gauge field” \mathcal{V}_μ is replaced by

$$\mathcal{V}_\mu = J\mu_q \delta_{\mu 0}, \quad (30)$$

with μ_q the quark number chemical potential introduced to access finite density.

In the vacuum the approximate Pauli-Gursey $SU(4)$ symmetry is further broken due to the VEV of chiral condensate $\langle \bar{\psi} \psi \rangle$, which is described by the appearance of a mean field of σ in our model. In addition, at finite μ_q it is possible that the diquark condensate $\langle \psi^T C \gamma_5 \tau_c^2 \tau_f^2 \psi \rangle$ emerges, leading to the baryon superfluidity that breaks the quark number conservation [27,28]. Such superfluidity is in our model triggered by a nonzero mean field of B (\bar{B}). In fact, once, in Eq. (27), one replaces σ and B^5 by their mean fields, which are real⁵:

$$\sigma_0 \equiv \langle \sigma \rangle, \quad \Delta \equiv \langle B^5 \rangle, \quad (31)$$

the effective potential with respect to σ_0 and Δ can be obtained as

$$\begin{aligned}
V_{\sigma_0, \Delta} &= -2\mu_q^2 \Delta^2 + \frac{m_0^2}{2} (\sigma_0^2 + \Delta^2) \\
&\quad + \frac{8\lambda_1 + 2\lambda_2 - c}{32} (\sigma_0^2 + \Delta^2)^2 - 2\sqrt{2} h_q \sigma_0.
\end{aligned} \quad (32)$$

It should be noted that both the mean fields σ_0 and Δ keep the parity and isospin symmetries intact.

The mass of each hadron can be determined by expanding the Lagrangian (27) up to quadratic order in the corresponding hadron field on top of the mean fields (31). We display their detailed expressions in Appendix A and here we only explain important features:

- (i) In the vacuum where $\mu_q = 0$ and naturally $\Delta = 0$, a mass difference between π and η is proportional to c that stems from the $U(1)_A$ axial anomaly as seen in Eq. (A21). In other words, in our model the mass of η is pushed up by the anomaly effect as observed from the KMT term in three-color QCD [74–77].

⁵In this phase choice for Δ , mean fields of B and \bar{B} become $\langle B \rangle = \langle \bar{B} \rangle = \Delta/\sqrt{2}$, and B^4 turns into the NG mode associated with the breakdown of baryon number symmetry.

- (ii) For $\lambda_1 = c = 0$,⁶ the vacuum masses of η , π , B , and \bar{B} , which belong to the same multiplet of $SU(4)$, are degenerate, and so are those of σ , a_0 , B' , and \bar{B}' [see Eqs. (A24) and (A25)]. These degeneracies indicate that effects of $SU(4)$ symmetry partly remain even when the symmetry is explicitly broken by current quark masses.
- (iii) In the baryon superfluid phase where Δ is nonzero, σ , B , and \bar{B} , whose spin and parity are $J^P = 0^+$, can mix. Similarly, η , B' , and \bar{B}' having $J^P = 0^-$ can mix in the superfluid phase. Such mixing stems from violation of baryon number conservation triggered by the diquark condensates. In fact, as can be seen from Eqs. (A15) and (A19) the corresponding mixing terms are proportional to Δ . However, the mixing terms happen to be proportional to σ_0 as well, and therefore at sufficiently large μ_q when the chiral condensate becomes small due to the approximate restoration of chiral symmetry, all mixings are small too.

The ground state is determined by stationary conditions of the potential (32) with respect to σ_0 and Δ . That is, the relevant mean fields must satisfy

$$m_0^2 + \frac{8\lambda_1 + 2\lambda_2 - c}{8}(\sigma_0^2 + \Delta^2) = \frac{2\sqrt{2}h_q}{\sigma_0}, \quad (33)$$

and

$$\left(-4\mu_q^2 + m_0^2 + \frac{8\lambda_1 + 2\lambda_2 - c}{8}(\sigma_0^2 + \Delta^2)\right)\Delta = 0, \quad (34)$$

respectively. Chiral symmetry or, more precisely, $SU(4)$ Pauli-Gursey symmetry, is explicitly broken due to the current-quark mass effect h_q , and hence the trivial solution of $\sigma_0 = 0$ denoting the $SU(4)$ symmetric phase does not satisfy Eq. (33). On the other hand, Eq. (34) possesses both the trivial and nontrivial solutions of Δ . The nontrivial solutions are selected by the value of chemical potential. In fact, once one inserts Eq. (33) into Eq. (34), the nontrivial Δ solution leads to

$$\mu_q^2 = \frac{h_q}{\sqrt{2}\sigma_0}, \quad (35)$$

which cannot hold for smaller μ_q . For adequately small μ_q , therefore, the nontrivial solution of Δ can be discarded and hence the baryon superfluid phase does not emerge as naively expected. The trivial solution $\Delta = 0$ leads to the hadronic phase, which is continuously connected to the system with vanishing μ_q . In the hadronic phase, according to Eq. (33), the value of σ_0 does not change from that in the

vacuum σ_0^{vac} . Note that the vacuum pion mass can be expressed as

$$(m_\pi^{\text{vac}})^2 = \frac{2\sqrt{2}h_q}{\sigma_0^{\text{vac}}} \quad (36)$$

from Eq. (A10). Then, the critical chemical potential μ_q^* for the baryon superfluid phase can be analytically evaluated as

$$\mu_q^* = \frac{m_\pi^{\text{vac}}}{2}, \quad (37)$$

from Eq. (35) with σ_0 being replaced by σ_0^{vac} . The critical chemical potential (37) is the same as the result of chiral perturbation theory [27,28] and NJL model [33],⁷ and suggested numerically by lattice simulations [5,14,18].

The baryonic density can be evaluated by taking a derivative of the potential $V_{\sigma_0, \Delta}$ with respect to μ_q :

$$\rho = -\frac{\partial V_{\sigma_0, \Delta}}{\partial \mu_q} = 4\Delta^2 \mu_q. \quad (38)$$

Therefore, the baryonic density arises above the critical chemical potential μ_q accompanied by the onset of baryon superfluidity, whereas in the hadronic phase ρ always vanishes. The latter constant behavior is related to the Silver Blaze property, which dictates the constancy of all thermodynamic quantities.

III. INPUTS

In order to fix the model parameters, in the present work we employ the recent lattice results for hadron mass spectrum [55,81], which ensures quantitatively convincing investigation.⁸ Results from the lattice simulation, which are in part still tentative, are summarized as follows:

- (i) In the physical unit, the pion mass is estimated to be $m_\pi = 738$ MeV with good accuracy.
- (ii) It seems that masses of π and η are almost identical in the hadronic phase, and hence we can take $c = 0$. This choice implies disappearance of $U(1)_A$ anomaly effect in the hadronic phase.⁹
- (iii) The measured masses of negative-parity baryons B' and \bar{B}' in the vacuum read $m_{B'(\bar{B}')}^{\text{vac}} = [1611 \pm 128(\text{stat})_{-678}^{+128}(\text{syst})]$ MeV. Taking the central

⁷It is expected that the critical chemical potential (37) holds to all orders in perturbation theory. In particular, Eq. (37) was proven at one-loop order explicitly in chiral perturbation theory [80].

⁸In Ref. [21], the physical scale is fixed by $T_c = 200$ MeV at $\mu_q = 0$, where T_c denotes the pseudocritical temperature of the chiral-phase transition.

⁹In the simulation contributions from disconnected diagrams are not included. Such effects however seem to be negligible [9,55].

⁶It corresponds to the leading approximation of the large N_c expansion [78,79] as shown in Appendix B.

value as $m_{B'(\bar{B}')}^{\text{vac}} \approx 1611$ MeV, we estimate a mass ratio of $B'(\bar{B}')$ and π to be $m_{B'(\bar{B}')}^{\text{vac}}/m_{\pi}^{\text{vac}} \approx 2.18$.¹⁰

- (iv) The computed mass of the 0^+ scalar meson in the hadronic phase is also accompanied by uncertainties. The results in the vacuum ($\mu_q = 0$) are quite noisy, but those at finite μ_q in the hadronic phase are rather worth using as inputs: $m_{\sigma} = [1453 \pm 84.7(\text{stat})_{-84.7}^{+103}(\text{syst})]$ MeV at $\mu_q = 119$ MeV and $m_{\sigma} = [1452 \pm 101(\text{stat})_{-106}^{+109}(\text{syst})]$ MeV at $\mu_q = 238$ MeV. From these values and the assumption that m_{σ} dose not change in the hadronic phase, we find $1.75 \lesssim m_{\sigma}^{\text{vac}}/m_{\pi}^{\text{vac}} \lesssim 2.2$.

From those lattice inputs we can fix m_0^2 , c , and h_q and also determine a range of λ_1 . In contrast, the dimensionless parameter λ_2 remains to be fixed. Then, we choose $\sigma_0^{\text{vac}} = 250$ MeV as a typical value to determine λ_2 in such a way that the magnitude of λ_2 becomes comparable to that broadly employed in the three-flavor linear sigma model [71–73]. The smaller (larger) value of σ_0^{vac} we take, the larger (smaller) value of λ_2 we obtain. We note that the choice of σ_0^{vac} does not affect the hadron mass spectrum at any μ_q as shown in Appendix B, as long as we stick to the large- N_c limit, i.e., $\lambda_1 = c = 0$. The VEV σ_0^{vac} is related to the pion decay constant f_{π} associated with the breakdown of $SU(4) \rightarrow Sp(4)$ as $f_{\pi} = \sigma_0^{\text{vac}}/\sqrt{2}$; f_{π} has yet to be measured on the lattice.

From the above procedure, the range of λ_1 is found to be $-7 \lesssim \lambda_1 \lesssim 0$, and hence for the numerical analysis in Sec. IV we consider two distinct cases $\lambda_1 = 0$ and $\lambda_1 = -7$ for clear discussions. The resultant parameters are summarized in the sets (I) and (II) in Table II. In the table, although the simulated mass spectrum favors $c = 0$, we also display the parameter set (III) with nonzero value of c to examine effects of the $U(1)_A$ axial anomaly on hadron mass spectrum, especially in the baryon superfluid phase later. Here, we again emphasize that the parameter set (I) where $\lambda_1 = c = 0$ is satisfied corresponds to the leading approximation of the large- N_c expansion.

Before moving on to numerical computations of the hadron mass spectrum, we plot μ_q dependence of σ_0 , Δ , and ρ in Fig. 1 with the parameter set (I) of Table II as a demonstration. The left panel depicts σ_0 (blue) and Δ (red) normalized by σ_0^{vac} , respectively, and the right one depicts the scaled baryonic density [5].

TABLE II. Parameter sets employed for computation of hadron mass spectrum in Sec. IV. The sets (I) and (II) are reasonable enough to reproduce the recent lattice results for hadron masses in the hadronic phase.

	c	λ_1	λ_2	m_0^2	h_q
Set (I)	0	0	65.6	$-(693 \text{ MeV})^2$	$(364 \text{ MeV})^3$
Set (II)	0	-7	65.6	$-(206 \text{ MeV})^2$	$(364 \text{ MeV})^3$
Set (III)	15	0	58.1	$-(495 \text{ MeV})^2$	$(364 \text{ MeV})^3$

$$\tilde{\rho} = \frac{\rho}{16f_{\pi}^2 m_{\pi}^{\text{vac}}}. \quad (39)$$

In the figure the vertical dotted line corresponds to the critical chemical potential μ_q^* given by Eq. (37), i.e., the transition between the hadronic and baryon superfluid phases. Figure 1 clearly exhibits the Silver Blaze property in the hadronic phase. Besides, the figure indicates that σ_0 decreases with μ_q in the baryon superfluid phase, resulting in the restoration of chiral symmetry at sufficiently high baryonic density. On the other hand, Δ increases monotonically as μ_q becomes large in the superfluid phase. Besides, unlike analysis from chiral perturbation theory within the mean-field approach where $\sigma_0^2 + \Delta^2 = (\text{constant})$ is satisfied for any value of μ_q [27,28],¹¹ the linear sigma model naturally violates such a conservation law. This is because the latter is based on the linear representation of quarks where the ground-state configuration is dynamically changed in accordance with the change of breaking strength of the Pauli-Gursey $SU(4)$ symmetry. A similar behavior is observed in the NJL model [33].

IV. MASS SPECTRUM

In this section we display the numerical results for μ_q dependence of the hadron masses evaluated in our present model. First, in Sec. IV A we present the resultant mass spectrum with the parameter sets (I) and (II) in Table II consistent with the recent lattice simulation. Next, in Sec. IV B we study the mass modifications with the set (III) in Table II to have a closer look at effects of the $U(1)_A$ axial anomaly especially in the baryon superfluid phase. Finally, in Sec. IV C, we discuss the chiral partner structure in our model with the set (I).

A. Results in the absence of $U(1)_A$ anomaly

Here, we investigate the hadron mass modifications for the parameter sets (I) and (II) in Table II, which are favored by the mass spectrum in the hadronic phase measured by

¹⁰The simulated values of $m_{B'}$ and $m_{\bar{B}'}$ at $\mu_q = 119$ MeV in the hadronic phase are $m_{B'} = [1238 \pm 87.6(\text{stat})_{-87.6}^{+112}(\text{syst})]$ MeV and $m_{\bar{B}'} = [1704 \pm 65.5(\text{stat})_{-71.0}^{+98.2}(\text{syst})]$ MeV, respectively. When estimating $m_{B'(\bar{B}')}^{\text{vac}} \approx 1611$ MeV, the mass formula that diquark baryons must satisfy in the hadronic phase, as will be shown in Eq. (40), reads $m_{B'} \approx 1373$ MeV and $m_{\bar{B}'} \approx 1849$ MeV at $\mu_q = 119$ MeV. Deviations between these theoretical values and the simulated values are not large unreasonably.

¹¹The relation $\sigma_0^2 + \Delta^2 = (\text{constant})$ is violated when loop corrections are taken into account, even in chiral perturbation theory.

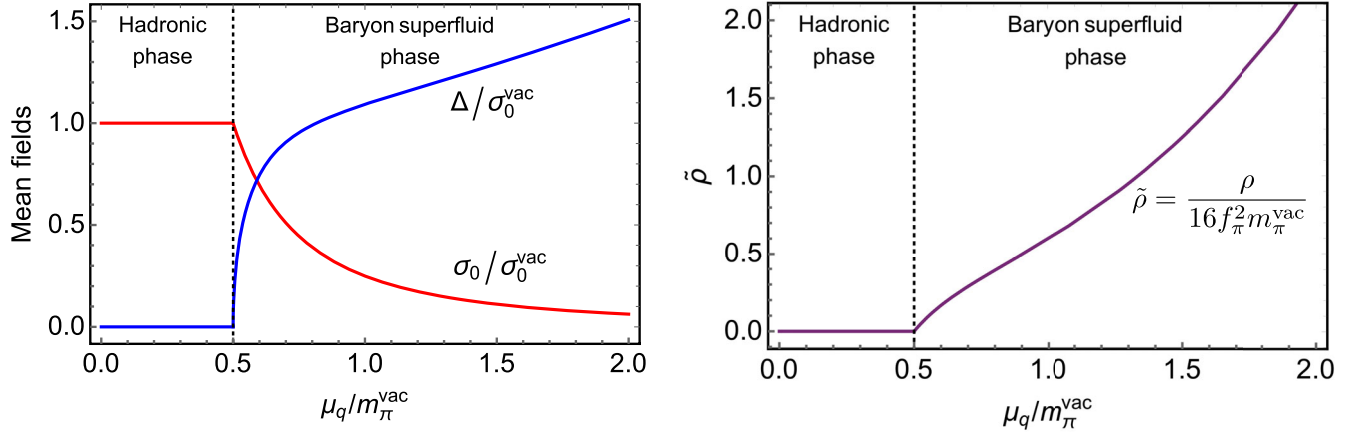


FIG. 1. The μ_q dependence of σ_0 and Δ (left panel) and that of the scaled baryonic density $\tilde{\rho}$ (right panel). The vertical line corresponds to $\mu_q^* = m_\pi^{\text{vac}}/2$, which distinguishes the normal and baryon superfluid phases.

the recent lattice simulation [55,81]. The sets are characterized by $c = 0$, where the $U(1)_A$ anomaly is absent.

Depicted in Fig. 2 is the resultant μ_q dependence of the hadron masses with the set (I). The left and right panels indicate the 0^+ (a_0 , σ , B , and \bar{B}) and 0^- (π , η , B' , and \bar{B}') hadron masses normalized by the vacuum pion mass m_π^{vac} , respectively, and the vertical dotted line for these panels corresponds to the critical chemical potential μ_q^* in Eq. (37). As can be seen from the figure, in the hadronic phase for $\mu_q < \mu_q^*$ the masses of mesons, which do not carry the baryon number, are unchanged while those of baryons and antibaryons monotonically change as

$$\begin{aligned} m_{B,B'} &= m_{B,B'}^{\text{vac}} - 2\mu_q, \\ m_{\bar{B},\bar{B}'} &= m_{\bar{B},\bar{B}'}^{\text{vac}} + 2\mu_q. \end{aligned} \quad (40)$$

These behaviors mean that in this phase the chemical potential μ_q simply shifts energy levels of the (anti)baryons

without being accompanied by medium effects. Such stable μ_q dependences are understandable by the absence of baryonic density as in the right panel of Fig. 1.

Here, we note that for the parameter set (I), not only the a_0 and σ masses but also the π and η ones are identical in the hadronic phase. The former is realized by the large- N_c condition $\lambda_1 = c = 0$, and the latter is solely by the neglect of $U(1)_A$ anomaly, i.e., $c = 0$ as already explained. These properties are clearly understood by Fig. 3, where the mass spectrum is obtained with the parameter set (II); the figure shows that the negative λ_1 acts to lower the σ mass, leading to breaking of the degeneracy of (a_0 , σ), while it does not destroy the mass degeneracy of (π , η). As a result, a level crossing between σ and \bar{B} takes place below the critical chemical potential μ_q^* . From the figure, it is also found that the positive λ_1 acts to increase the σ mass to break the degeneracy of a_0 and σ .

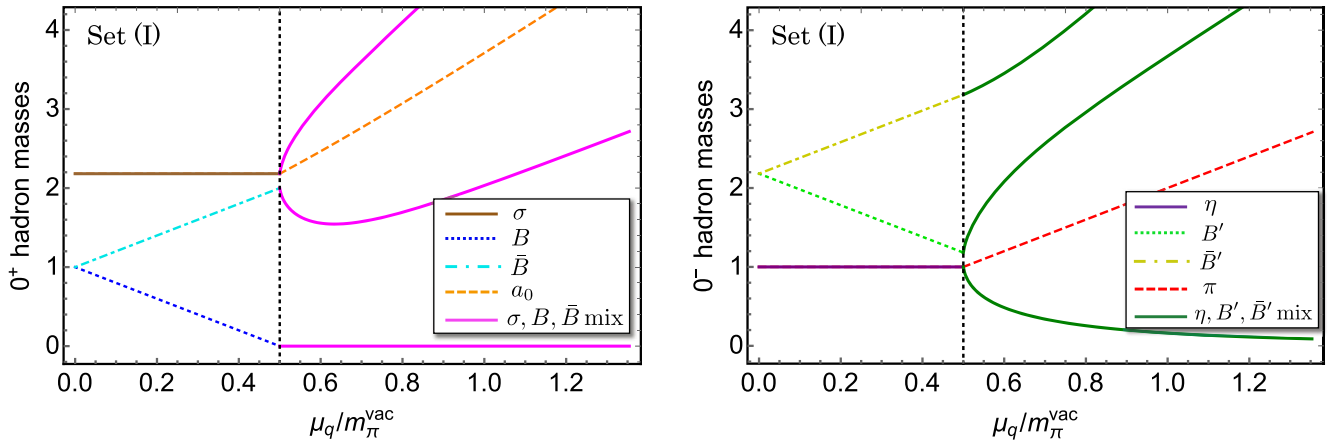


FIG. 2. Left and right panels represent the μ_q dependence of 0^+ hadron masses (a_0 , σ , B , and \bar{B}) and that of 0^- hadron masses (π , η , B' , and \bar{B}'), respectively, calculated with the parameter set (I). These hadron masses are normalized by the vacuum pion mass m_π^{vac} . The vertical dotted line corresponds to the critical chemical potential μ_q^* .

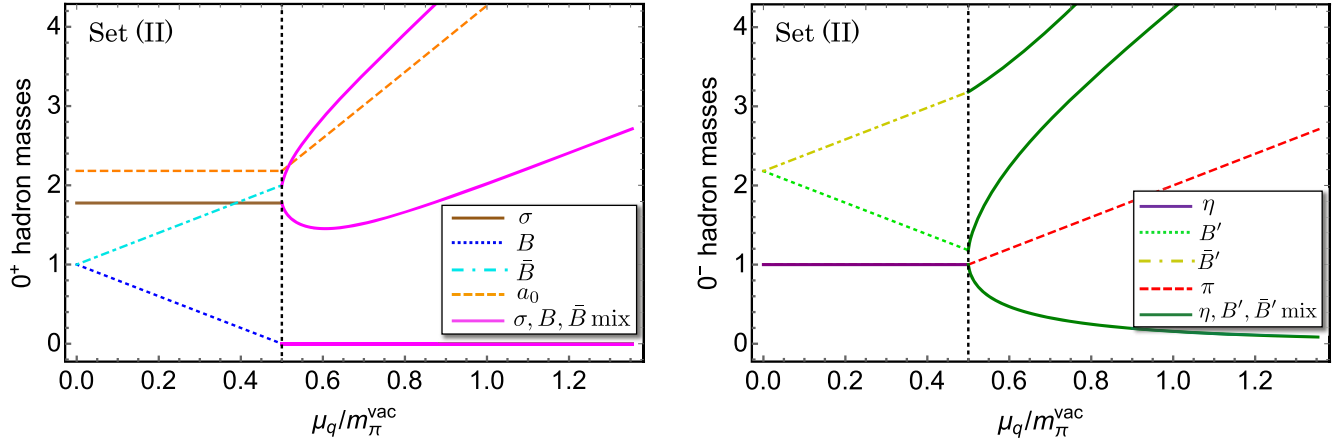


FIG. 3. Same as Fig. 2 but with the parameter set (II).

In the baryon superfluid phase at $\mu_q > \mu_q^*$ in Figs. 2 and 3, due to the violation of baryon number conservation several nontrivial mass modifications are found. First, for $J^P = 0^+$ hadrons, σ , B , and \bar{B} mix, and the lowest branch becomes massless, which plays the role of the NG boson associated with the violation of $U(1)_B$ baryon number symmetry. The isotriplet a_0 meson does not join the mixing since the $SU(2)$ isospin symmetry is not broken by Δ . Next, for $J^P = 0^-$ hadrons, η , B' , and \bar{B}' also mix to draw a complicated mass spectrum. Due to the level repulsion among them, the lowest branch is pushed down and its mass becomes smaller than m_π^{vac} . Such remarkable behaviors of the lowest branches are certainly observed in the recent lattice simulation [55,81]. Comparing Figs. 2 and 3, we can see that in the baryon superfluid phase the negative λ_1 acts to slightly increase the mass of a_0 and that of the second-lowest branch of the η - B' - \bar{B}' mixed state. The mass orderings in the superfluid phase are nevertheless identical for the sets (I) and (II). For $\lambda_1 = c = 0$, it should be noted that the lowest branch of the η - B' - \bar{B}' mixed state is reduced to a massless mode at sufficiently large μ_q . In Sec. IV C we will come back to this point.

In addition to the above findings, interestingly enough, the μ_q dependence of the π mass in the baryon superfluid phase is found to be expressed as

$$m_\pi^2 = 4\mu_q^2, \quad (41)$$

which is the same as that predicted by chiral perturbation theory and the NJL model [27,28,33]. The mass formula (41) is analytically derived for any parameter set in the present model.

B. Effects of the $U(1)_A$ anomaly

As mentioned above, the mass spectrum in the hadronic phase measured by the recent lattice simulation supports the absence of $U(1)_A$ anomaly. Even so, it is useful to study the hadron mass spectrum at finite μ_q in the case in which the anomaly is present. For this reason, in this subsection we work with the parameter set (III).

Depicted in Fig. 4 is the result with the set (III). In the hadronic phase, the $U(1)_A$ anomaly effect with $c > 0$ pushes down the σ mass and pushes up the η mass,

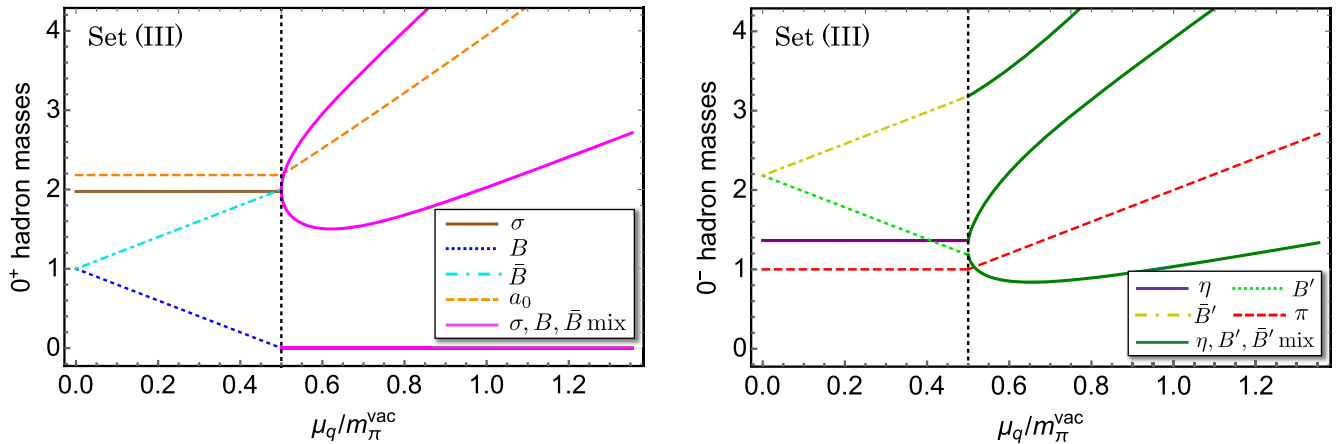


FIG. 4. Same as Fig. 2 but with the parameter set (III).

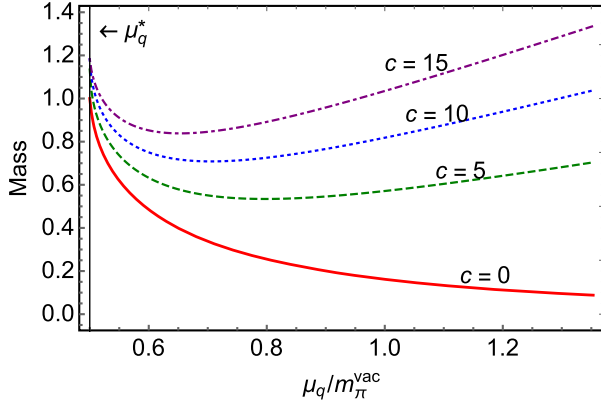


FIG. 5. The μ_q dependence of the mass of the lowest branch of the η - B' - \bar{B}' mixed state in the baryon superfluid phase calculated for several c 's. The mass is normalized by m_π^{vac} .

resulting in breaking of mass degeneracies of (a_0, σ) and of (π, η) . As a result, level crossings of \bar{B} and σ for 0^+ hadrons and of B' and η for 0^- ones can occur below μ_q^* . In the baryon superfluid phase, the mass spectrum is mostly similar to the one presented with the parameter sets (I) and (II) except the lowest branch of the η - B' - \bar{B}' mixed state; notably the mass reduction of the state observed in Figs. 2 and 3 is tempered, and the mass again increases gradually well above μ_q^* . Such a characteristic behavior is obviously distinct from the $c = 0$ case where the mass reduction is striking and becomes asymptotically zero. Therefore, we conclude that such weakened mass reduction can be a useful signal to measure the change of the magnitude of the $U(1)_A$ anomaly in the superfluid phase.

In order to have a closer look at the influence of the $U(1)_A$ anomaly on the mass of the lowest branch of the η - B' - \bar{B}' mixed state, we depict μ_q dependence of its mass in the baryon superfluid phase for several values of c with λ being set to zero in Fig. 5. From the figure one can see that the mass is strongly affected by the value of c , i.e., the magnitude of the $U(1)_A$ anomaly. In particular, when $c > 0$ the mass is proportional to μ_q in the limit of $\mu_q \rightarrow \infty$, while only when $c = 0$ the mass is reduced to zero in this limit.

C. Chiral partner structures

One of the characteristic features of the conventional linear sigma model is manifestation of the so-called chiral partner structure [57]. That is, the linear representation of hadrons allows us to explore how the mass degeneracy occurs among hadrons having opposite parities via axial transformations at the chiral restoration point. In order to identify the mass degeneracy structure at large μ_q , in this subsection we study the positive and negative parity hadrons simultaneously.

We display the μ_q dependence of all the hadron masses treated in the present model in Fig. 6. In this figure, we employ the parameter set (I) where the large- N_c limit is

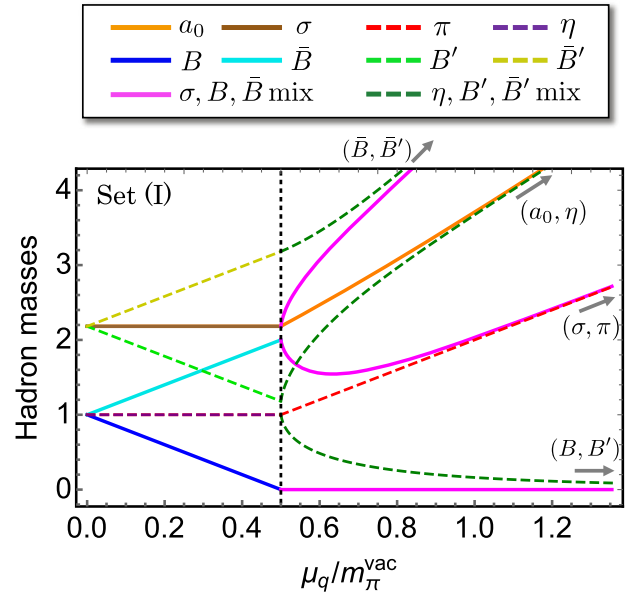


FIG. 6. The μ_q dependence of all the normalized hadron masses calculated with the parameter set (I). The solid and dashed curves denote the positive and negative parity hadrons, respectively, and the vertical dotted line corresponds to μ_q^* . The two states indicated in each parenthesis are the respective chiral partners realized at sufficiently large μ_q .

taken as the most instructive choice. The solid curves and dashed curves denote the positive and negative parity hadrons, respectively, and the vertical dotted line corresponds to μ_q^* . Figure 6 clearly shows that each state can be classified by asymptotic mass degeneracy as a chiral partner of the degenerate pair. Analytically, once one takes $\sigma_0 \rightarrow 0$ at large μ_q and sets $\lambda_1 = c = 0$ in the mass formulas in Appendix A, the troublesome mixing disappears and one can easily find

$$\begin{aligned} m_B^2 &= m_{B'}^2 = 0, \\ m_\sigma^2 &= m_\pi^2 = \mu_q^2, \\ m_{a_0}^2 &= m_\eta^2 = 12\mu_q^2, \\ m_{\bar{B}}^2 &= m_{\bar{B}'}^2 = 24\mu_q^2, \end{aligned} \quad (42)$$

which are independent of λ_2 . The asymptotic mass formula (42) clearly exhibits the chiral partner structure. In particular, the formula indicates that the partners are (B, B') , (σ, π) , (a_0, η) , and (\bar{B}, \bar{B}') from the lowest mass, a sequence expected from the $SU(2)_A$ axial transformations. It should be noted that the chiral partner structures for baryons (B, B') and antibaryons (\bar{B}, \bar{B}') are realized only when the $U(1)_A$ anomaly effect is switched off, i.e., $c = 0$, and the large- N_c limit is taken, i.e., $\lambda_1 = c = 0$, respectively.

The predicted mass degeneracies are expected to provide useful information of chiral symmetric properties of the hadrons at dense regime for future lattice simulations.

V. CONCLUSIONS

In this article, motivated by the recent lattice simulation [55,81], we have investigated hadron mass modifications at finite quark chemical potential μ_q in QC_2D with two flavors within the linear sigma model. The model enables us to study not only the masses of the ground-state pseudoscalar mesons and scalar diquark baryons but also those of the chiral partners carrying opposite parities, which is the notable advantage of employing the linear sigma model. That is, we have succeeded in treating the positive parity mesons and diquark baryons: σ , a_0 , B , and \bar{B} , and the negative parity ones: η , π , B' , and \bar{B}' , in a unified way.

In order to fix the model parameters, we have used the lattice results for hadron mass spectrum in the hadronic phase where the diquark condensate does not emerge [55,81]. In particular, the lattice result suggests that masses of π and η are identical in the hadronic phase, implying that effects of the $U(1)_A$ axial anomaly are suppressed there. Within our present model, such a suppression has been described by omitting the KMT-type contributions.

In the baryon superfluid phase where the diquark condensate emerges, we have found a rich mass spectrum involving the mixing among σ - B - \bar{B} for $J^P = 0^+$ hadrons and that among η - B' - \bar{B}' for $J^P = 0^-$ ones, which is triggered by the $U(1)_B$ baryon number violation. The former mixing plays an essential role in describing the massless nature of the NG boson in association with the violation of $U(1)_B$ baryon number symmetry, while the latter leads to a noteworthy mass reduction of the lowest branch of the η - B' - \bar{B}' mixed state. These characteristic properties have been indeed observed by the lattice simulation.

Besides, at sufficiently large μ_q , we have demonstrated the chiral partner structure by deriving mass degeneracies of the hadrons that have opposite parities and are connected by the axial transformations. The predicted mass degeneracies are expected to be useful as guides for future lattice simulations toward elucidation of influence of the chiral restoration on the hadron properties, i.e., elucidation of the hadron mass generation.

In the absence of the $U(1)_A$ anomaly, the mass reduction of the lowest branch of the η - B' - \bar{B}' mixed state is striking and the state finally becomes massless to exhibit the chiral partner structure with the NG boson. When the anomaly is present, the mass reduction is tempered such that the corresponding chiral partner structure is broken. The lattice simulation implies the latter tempered reduction. If this is the case, the $U(1)_A$ anomaly effects which are negligible in the hadronic phase possibly become sizable in the baryon superfluid phase. In this regard, we have also clarified a relation between the tempered mass reduction and the strength of the KMT determinant term. The relation is

expected to be useful to derive the change of the magnitude of anomaly effects from further lattice simulations. Meanwhile, within effective models, the increment of the anomaly in medium measured by the magnitude of the KMT determinant term in three-color QCD was indeed reported in Refs. [64,65,82]. Thus, we leave investigation on the strengthened anomaly effect in dense QC_2D matter for future study.

In what follows, we comment on relations between QC_2D and three-color QCD by focusing on the diquarks. In three-color QCD, diquarks themselves are not observable since they are not color singlets. Instead, singly heavy baryons consisting of one heavy quark and one diquark can be regarded as the corresponding hadrons to the diquark baryons in QC_2D . In three-color QCD, when one looks at the singly charmed baryons, the ground state is the well-established $\Lambda_c(2286)$ [83] (counterpart of B in QC_2D) but its chiral partner carrying a negative parity $\Lambda_c(\frac{1}{2}^-)$ (counterpart of B' in QC_2D) has not yet been observed experimentally despite theoretical predictions [84–90]. For this reason, seeking for $\Lambda_c(\frac{1}{2}^-)$ is one of the challenging topics on singly heavy baryon spectroscopy. On the other hand, in QC_2D the mass of negative-parity diquark B (\bar{B}) has been certainly measured by the lattice simulation. However, the pion mass is rather heavy such that B' (\bar{B}') becomes stable. Therefore, numerical investigation of the hadrons in QC_2D by changing the pion mass, especially via dynamical aspects of B' (\bar{B}'), would be desired to give clues to unveil problems on hidden $\Lambda_c(\frac{1}{2}^-)$ in three-color QCD. In addition, from further numerical elucidation of modifications of diquark baryons at finite density in QC_2D , it is expected that our deeper understanding of medium corrections of singly heavy baryons from a symmetry point of view would be achieved.

ACKNOWLEDGMENTS

The authors thank Makoto Oka for useful discussions. D.S. is supported by the RIKEN special postdoctoral researcher program. K.M. is supported in part by the Japan Society for the Promotion of Science (JSPS). E.I. is supported by JSPS KAKENHI with Grant No. 19K03875, JST PRESTO Grant No. JPMJPR2113, JSPS Grant-in-Aid for Transformative Research Areas Grant No. (A) JP21H05190, and JST Grant No. JPMJPF2221. K.I. is supported by JSPS KAKENHI with Grant No. 18H05406. The lattice Monte Carlo simulation is supported by the High-Performance Computing Infrastructure-Joint Usage/Research Center for Interdisciplinary Large-scale Information Infrastructures (HPCI-JHPCN) System Research Project (Project ID No. jh220021).

APPENDIX A: HADRON MASSES AT FINITE μ_q

Here, we show mass terms of the hadrons treated in our linear sigma model.

The mass terms are provided by expanding the Lagrangian (27) up to quadratic order in the hadron fields, on top of the mean fields (31). The resultant Lagrangian reads

$$\begin{aligned} \mathcal{L} = & \mathcal{L}_B + \mathcal{L}_\sigma + \mathcal{L}_{B\sigma} + \mathcal{L}_{B'} + \mathcal{L}_\eta + \mathcal{L}_{B'\eta} \\ & + \mathcal{L}_{a_0} + \mathcal{L}_\pi + \cdots, \end{aligned} \quad (\text{A1})$$

where

$$\begin{aligned} \mathcal{L}_B = & \frac{1}{2} \partial_\mu B_4 \partial^\mu B_4 + \frac{1}{2} \partial_\mu B_5 \partial^\mu B_5 + 2\mu_q (\partial_0 B_4 B_5 \\ & - B_4 \partial_0 B_5) - \frac{m_{B_4}^2}{2} B_4^2 - \frac{m_{B_5}^2}{2} B_5^2, \end{aligned} \quad (\text{A2})$$

$$\mathcal{L}_\sigma = \frac{1}{2} \partial_\mu \sigma \partial^\mu \sigma - \frac{m_\sigma^2}{2} \sigma^2, \quad (\text{A3})$$

$$\mathcal{L}_{B\sigma} = -m_{B_5\sigma}^2 \sigma B_5, \quad (\text{A4})$$

$$\begin{aligned} \mathcal{L}_{B'} = & \frac{1}{2} \partial_\mu B'_4 \partial^\mu B'_4 + \frac{1}{2} \partial_\mu B'_5 \partial^\mu B'_5 + 2\mu_q (\partial_0 B'_4 B'_5 \\ & - B'_4 \partial_0 B'_5) - \frac{m_{B'_4}^2}{2} B'^2_4 - \frac{m_{B'_5}^2}{2} B'^2_5, \end{aligned} \quad (\text{A5})$$

$$\mathcal{L}_\eta = \frac{1}{2} \partial_\mu \eta \partial^\mu \eta - \frac{m_\eta^2}{2} \eta^2, \quad (\text{A6})$$

$$\mathcal{L}_{B'\eta} = -m_{B'_5\eta}^2 B'_5 \eta, \quad (\text{A7})$$

$$\mathcal{L}_{a_0} = \frac{1}{2} \partial_\mu a_0^a \partial^\mu a_0^a - \frac{m_{a_0}^2}{2} a_0^a a_0^a \quad (a = 1, 2, 3), \quad (\text{A8})$$

and

$$\mathcal{L}_\pi = \frac{1}{2} \partial_\mu \pi^a \partial^\mu \pi^a - \frac{m_\pi^2}{2} \pi^a \pi^a \quad (a = 1, 2, 3), \quad (\text{A9})$$

with the corresponding masses

$$m_\pi^2 = m_0^2 + \frac{8\lambda_1 + 2\lambda_2 - c}{8} (\sigma_0^2 + \Delta^2), \quad (\text{A10})$$

$$m_{a_0}^2 = m_\pi^2 + \frac{\lambda_2}{2} (\sigma_0^2 + \Delta^2) + \frac{c}{4} (\sigma_0^2 + \Delta^2), \quad (\text{A11})$$

$$m_{B_4}^2 = m_\pi^2 - 4\mu_q^2, \quad (\text{A12})$$

$$m_{B_5}^2 = m_\pi^2 - 4\mu_q^2 + \frac{8\lambda_1 + 2\lambda_2 - c}{4} \Delta^2, \quad (\text{A13})$$

$$m_\sigma^2 = m_\pi^2 + \frac{8\lambda_1 + 2\lambda_2 - c}{4} \sigma_0^2, \quad (\text{A14})$$

$$m_{B_5\sigma}^2 = \frac{8\lambda_1 + 2\lambda_2 - c}{4} \sigma_0 \Delta, \quad (\text{A15})$$

$$m_{B'_4}^2 = m_\pi^2 - 4\mu_q^2 + \frac{2\lambda_2 + c}{4} (\sigma_0^2 + \Delta^2), \quad (\text{A16})$$

$$m_{B'_5}^2 = m_\pi^2 - 4\mu_q^2 + \frac{\lambda_2}{2} \sigma_0^2 + \frac{c}{4} (\sigma_0^2 + 2\Delta^2), \quad (\text{A17})$$

$$m_\eta^2 = m_\pi^2 + \frac{\lambda_2}{2} \Delta^2 + \frac{c}{4} (2\sigma_0^2 + \Delta^2), \quad (\text{A18})$$

and

$$m_{B'_5\eta}^2 = \frac{2\lambda_2 - c}{4} \sigma_0 \Delta. \quad (\text{A19})$$

Equations (A4) and (A7) tell us that not only σ , B , and \bar{B} but also η , B' , and \bar{B}' can mix in the baryon superfluid phase where $\Delta \neq 0$, due to the violation of baryon number conservation. In fact, as can be seen from Eqs. (A15) and (A19) those mixing terms are proportional to Δ .

In order to examine the detailed structure of hadron masses in our model, we focus on the vacuum described by $\mu_q = 0$ with $\sigma_0 = \sigma_0^{\text{vac}}$ and $\Delta = 0$. The resultant hadron masses read

$$(m_\pi^{\text{vac}})^2 = (m_{B_4}^{\text{vac}})^2 = (m_{B_5}^{\text{vac}})^2, \quad (\text{A20})$$

$$(m_\eta^{\text{vac}})^2 = (m_\pi^{\text{vac}})^2 + \frac{c}{2} (\sigma_0^{\text{vac}})^2, \quad (\text{A21})$$

$$\begin{aligned} (m_{a_0}^{\text{vac}})^2 &= (m_{B'_4}^{\text{vac}})^2 = (m_{B'_5}^{\text{vac}})^2 \\ &= (m_\pi^{\text{vac}})^2 + \frac{2\lambda_2 + c}{4} (\sigma_0^{\text{vac}})^2, \end{aligned} \quad (\text{A22})$$

$$(m_\sigma^{\text{vac}})^2 = (m_\pi^{\text{vac}})^2 + \frac{8\lambda_1 + 2\lambda_2 - c}{4} (\sigma_0^{\text{vac}})^2. \quad (\text{A23})$$

Equation (A21) implies that in the vacuum the mass difference between η and π is proportional to c and thus stems from the $U(1)_A$ anomaly. Typically the η meson is heavier than π , so in this case $c > 0$. Besides, when assuming the large- N_c limit, i.e., $\lambda_1 = c = 0$, we can find

$$(m_\eta^{\text{vac}})^2 = (m_\pi^{\text{vac}})^2 = (m_{B_4}^{\text{vac}})^2 = (m_{B_5}^{\text{vac}})^2, \quad (\text{A24})$$

and

$$(m_\sigma^{\text{vac}})^2 = (m_{a_0}^{\text{vac}})^2 = (m_{B'_4}^{\text{vac}})^2 = (m_{B'_5}^{\text{vac}})^2. \quad (\text{A25})$$

APPENDIX B: THE N_c COUNTING

In this appendix, we give explanations of our N_c counting of the model parameters and also clarify how hadron masses depend on the value of σ_0^{vac} .

As is well known, diagrams in the mesonic level are of $\mathcal{O}(N_c)$ since the leading contributions are scaled in the

same way as a simple quark loop when the gauge coupling g_c is scaled as $N_c^{-1/2}$. Meanwhile, wave functions of the mesons are of $\mathcal{O}(\sqrt{N_c})$ [78,79]. Thus, the N_c counting of coupling constants in effective models involving n mesons is estimated to be of $\mathcal{O}(N_c^{(2-n)/2})$ [73]. Within this N_c counting, m_0^2 and λ_2 behave as $m_0^2 = \mathcal{O}(N_c^0)$ and $\lambda_2 = \mathcal{O}(N_c^{-1})$, respectively. The other four-point coupling λ_1 is, however, scaled as N_c^{-2} since the λ_1 term includes two traces with respect to flavors; the leading contributions cannot be described by one quark loop but by two loops mediated by gluons in between. Phenomenologically, such an N_c suppression is referred to as the Zweig rule. Besides, the constant h_q , which is responsible for the explicit breaking of the Pauli-Gursey $SU(4)$ symmetry, is $h_q = \mathcal{O}(N_c^{1/2})$, and σ_0 is of $\mathcal{O}(N_c^{1/2})$. By combining these N_c countings with Eqs. (35), (36), and (41), the pion mass in both the vacuum and medium can be understood to be of $\mathcal{O}(N_c^0)$ as expected.

The N_c counting of the anomalous contribution c can be determined by focusing on the η mass formula in the vacuum. As discussed in Ref. [78], the η mass must be scaled as $N_c^{-1/2}$ in such a way that the η meson turns into an NG boson in association with the suppression of the $U(1)_A$ anomaly. Therefore, we can conclude from Eq. (A21) that c is scaled as N_c^{-2} .

To summarize, our N_c counting of the model parameters is determined as

$$\begin{aligned} m_0^2 &= \mathcal{O}(N_c^0), & \lambda_1 &= \mathcal{O}(N_c^{-2}), & \lambda_2 &= \mathcal{O}(N_c^{-1}), \\ h_q &= \mathcal{O}(N_c^{1/2}), & c &= \mathcal{O}(N_c^{-2}). \end{aligned} \quad (\text{B1})$$

Therefore, the parameter set with $\lambda_1 = c = 0$ corresponds to the large- N_c limit in which higher-order contributions can be discarded.

In the large- N_c limit where $\lambda_1 = c = 0$, one notable universal behavior of the hadron mass spectrum at finite μ_q can be derived. In this limit, from the stationary conditions for σ_0 and Δ in Eqs. (33) and (34), the nontrivial solutions are found to satisfy

$$\begin{aligned} \lambda_2 \sigma_0^2 &= \left(\frac{m_\pi^{\text{vac}}}{m_\pi} \right)^4 \lambda_2 (\sigma_0^{\text{vac}})^2, \\ \lambda_2 \Delta^2 &= \left(1 - \frac{(m_\pi^{\text{vac}})^2}{m_\pi^2} \right) [\lambda_2 (\sigma_0^{\text{vac}})^2 + 4m_\pi^2], \end{aligned} \quad (\text{B2})$$

respectively. That is, when we take m_π^{vac} and $m_{B'(\bar{B}')}^{\text{vac}}$ as inputs,

$$\lambda_2 (\sigma_0^{\text{vac}})^2 = 2(m_{B'(\bar{B}')}^{\text{vac}})^2 - 2(m_\pi^{\text{vac}})^2 = (\text{constant}) \quad (\text{B3})$$

holds from Eq. (A22), and accordingly $\lambda_2 \sigma_0^2$ and $\lambda_2 \Delta^2$ depend only on μ_q as can be seen from Eq. (B2) with $m_\pi^2 = 4\mu_q^2$. On the other hand, the mass formulas (A10)–(A19) become dependent only on $\lambda_2 \sigma_0^2$ and $\lambda_2 \Delta^2$ for $\lambda_1 = c = 0$. Therefore, the hadron masses in the baryon superfluid phase turn out to be dependent on μ_q alone in the large- N_c limit and hence unaffected by the vacuum value σ_0^{vac} . In other words, the hadron mass spectrum in both the hadronic and baryon superfluid phases is independent of the choice of σ_0^{vac} in the limit of interest here.

-
- [1] Shin Muroya, Atsushi Nakamura, Chiho Nonaka, and Tetsuya Takaishi, Lattice QCD at finite density: An introductory review, *Prog. Theor. Phys.* **110**, 615 (2003).
 - [2] Gert Aarts, Introductory lectures on lattice QCD at nonzero baryon number, *J. Phys. Conf. Ser.* **706**, 022004 (2016).
 - [3] Simon Hands, John B. Kogut, Maria-Paola Lombardo, and Susan E. Morrison, Symmetries and spectrum of $SU(2)$ lattice gauge theory at finite chemical potential, *Nucl. Phys.* **B558**, 327 (1999).
 - [4] J. B. Kogut, D. K. Sinclair, S. J. Hands, and S. E. Morrison, Two color QCD at nonzero quark number density, *Phys. Rev. D* **64**, 094505 (2001).
 - [5] Simon Hands, Istvan Montvay, Luigi Scorzato, and Jonivar Skullerud, Diquark condensation in dense adjoint matter, *Eur. Phys. J. C* **22**, 451 (2001).
 - [6] Shin Muroya, Atsushi Nakamura, and Chiho Nonaka, Behavior of hadrons at finite density: Lattice study of color $SU(2)$ QCD, *Phys. Lett. B* **551**, 305 (2003).
 - [7] Shailesh Chandrasekharan and Fu-Jiun Jiang, Phase diagram of two-color lattice QCD in the chiral limit, *Phys. Rev. D* **74**, 014506 (2006).
 - [8] Simon Hands, Seyong Kim, and Jon-Ivar Skullerud, Deconfinement in dense 2-color QCD, *Eur. Phys. J. C* **48**, 193 (2006).
 - [9] Simon Hands, Peter Sitch, and Jon-Ivar Skullerud, Hadron spectrum in a two-colour baryon-rich medium, *Phys. Lett. B* **662**, 405 (2008).
 - [10] Simon Hands, Seyong Kim, and Jon-Ivar Skullerud, A quarkyonic phase in dense two color matter?, *Phys. Rev. D* **81**, 091502 (2010).
 - [11] Seamus Cotter, Pietro Giudice, Simon Hands, and Jon-Ivar Skullerud, Towards the phase diagram of dense two-color matter, *Phys. Rev. D* **87**, 034507 (2013).
 - [12] Simon Hands, Seyong Kim, and Jon-Ivar Skullerud, Non-relativistic spectrum of two-color QCD at non-zero baryon density, *Phys. Lett. B* **711**, 199 (2012).

- [13] Tamer Boz, Seamus Cotter, Leonard Fister, Dhagash Mehta, and Jon-Ivar Skullerud, Phase transitions and gluodynamics in 2-colour matter at high density, *Eur. Phys. J. A* **49**, 87 (2013).
- [14] V. V. Braguta, E. M. Ilgenfritz, A. Yu. Kotov, A. V. Molochkov, and A. A. Nikolaev, Study of the phase diagram of dense two-color QCD within lattice simulation, *Phys. Rev. D* **94**, 114510 (2016).
- [15] M. Puhr and P. V. Buividovich, Numerical Study of Non-perturbative Corrections to the Chiral Separation Effect in Quenched Finite-Density QCD, *Phys. Rev. Lett.* **118**, 192003 (2017).
- [16] Tamer Boz, Ouraman Hajizadeh, Axel Maas, and Jon-Ivar Skullerud, Finite-density gauge correlation functions in QC2D, *Phys. Rev. D* **99**, 074514 (2019).
- [17] N. Yu. Astrakhantsev, V. G. Bornyakov, V. V. Braguta, E. M. Ilgenfritz, A. Yu. Kotov, A. A. Nikolaev, and A. Rothkopf, Lattice study of static quark-antiquark interactions in dense quark matter, *J. High Energy Phys.* **05** (2019) 171.
- [18] Kei Iida, Etsuko Itou, and Tong-Gyu Lee, Two-colour QCD phases and the topology at low temperature and high density, *J. High Energy Phys.* **01** (2020) 181.
- [19] Jonas Wilhelm, Lukas Holicki, Dominik Smith, Björn Wellegehausen, and Lorenz von Smekal, Continuum Goldstone spectrum of two-color QCD at finite density with staggered quarks, *Phys. Rev. D* **100**, 114507 (2019).
- [20] P. V. Buividovich, D. Smith, and L. von Smekal, Numerical study of the chiral separation effect in two-color QCD at finite density, *Phys. Rev. D* **104**, 014511 (2021).
- [21] Kei Iida, Etsuko Itou, and Tong-Gyu Lee, Relative scale setting for two-color QCD with $N_f = 2$ Wilson fermions, *Prog. Theor. Exp. Phys.* **2021**, 013B05 (2021).
- [22] N. Astrakhantsev, V. V. Braguta, E. M. Ilgenfritz, A. Yu. Kotov, and A. A. Nikolaev, Lattice study of thermodynamic properties of dense QC₂D, *Phys. Rev. D* **102**, 074507 (2020).
- [23] V. G. Bornyakov, V. V. Braguta, A. A. Nikolaev, and R. N. Rogalyov, Effects of dense quark matter on gluon propagators in lattice QC₂D, *Phys. Rev. D* **102**, 114511 (2020).
- [24] P. V. Buividovich, D. Smith, and L. von Smekal, Electric conductivity in finite-density $SU(2)$ lattice gauge theory with dynamical fermions, *Phys. Rev. D* **102**, 094510 (2020).
- [25] P. V. Buividovich, D. Smith, and L. von Smekal, Static magnetic susceptibility in finite-density $SU(2)$ lattice gauge theory, *Eur. Phys. J. A* **57**, 293 (2021).
- [26] Kei Iida and Etsuko Itou, Velocity of sound beyond the high-density relativistic limit from lattice simulation of dense two-color QCD, *Prog. Theor. Exp. Phys.* **2022**, 111B01 (2022).
- [27] J. B. Kogut, Misha A. Stephanov, and D. Toublan, On two color QCD with baryon chemical potential, *Phys. Lett. B* **464**, 183 (1999).
- [28] J. B. Kogut, Misha A. Stephanov, D. Toublan, J. J. M. Verbaarschot, and A. Zhitnitsky, QCD—Like theories at finite baryon density, *Nucl. Phys. B* **582**, 477 (2000).
- [29] J. T. Lenaghan, F. Sannino, and K. Splittorff, The superfluid and conformal phase transitions of two color QCD, *Phys. Rev. D* **65**, 054002 (2002).
- [30] Takuya Kanazawa, Tilo Wettig, and Naoki Yamamoto, Chiral Lagrangian and spectral sum rules for dense two-color QCD, *J. High Energy Phys.* **08** (2009) 003.
- [31] Prabal Adhikari, Soma B. Beleznyay, and Massimo Mannarelli, Finite density two color chiral perturbation theory revisited, *Eur. Phys. J. C* **78**, 441 (2018).
- [32] Masayasu Harada, Chiho Nonaka, and Tetsuro Yamaoka, Masses of vector bosons in two-color dense QCD based on the hidden local symmetry, *Phys. Rev. D* **81**, 096003 (2010).
- [33] Claudia Ratti and Wolfram Weise, Thermodynamics of two-colour QCD and the Nambu Jona-Lasinio model, *Phys. Rev. D* **70**, 054013 (2004).
- [34] Gao-feng Sun, Lianyi He, and Pengfei Zhuang, BEC-BCS crossover in the Nambu-Jona-Lasinio model of QCD, *Phys. Rev. D* **75**, 096004 (2007).
- [35] Kenji Fukushima and Kei Iida, Larkin-Ovchinnikov-Fulde-Ferrell state in two-color quark matter, *Phys. Rev. D* **76**, 054004 (2007).
- [36] Tomas Brauner, Kenji Fukushima, and Yoshimasa Hidaka, Two-color quark matter: $U(1)(A)$ restoration, superfluidity, and quarkyonic phase, *Phys. Rev. D* **80**, 074035 (2009); **81**, 119904(E) (2010).
- [37] Jens O. Andersen and Tomas Brauner, Phase diagram of two-color quark matter at nonzero baryon and isospin density, *Phys. Rev. D* **81**, 096004 (2010).
- [38] Tian Zhang, Tomas Brauner, and Dirk H. Rischke, QCD-like theories at nonzero temperature and density, *J. High Energy Phys.* **06** (2010) 064.
- [39] Lianyi He, Nambu-Jona-Lasinio model description of weakly interacting Bose condensate and BEC-BCS crossover in dense QCD-like theories, *Phys. Rev. D* **82**, 096003 (2010).
- [40] Shotaro Imai, Hiroshi Toki, and Wolfram Weise, Quark-hadron matter at finite temperature and density in a two-color PNJL model, *Nucl. Phys. A* **913**, 71 (2013).
- [41] Dyana C. Duarte, P. G. Allen, R. L. S. Farias, Pedro H. A. Manso, Rudnei O. Ramos, and N. N. Scoccola, BEC-BCS crossover in a cold and magnetized two color NJL model, *Phys. Rev. D* **93**, 025017 (2016).
- [42] Jingyi Chao, Phase diagram of two-color QCD matter at finite baryon and axial isospin densities, *Chin. Phys. C* **44**, 034108 (2020).
- [43] T. G. Khunjua, K. G. Klimenko, and R. N. Zhokhov, The dual properties of chiral and isospin asymmetric dense quark matter formed of two-color quarks, *J. High Energy Phys.* **06** (2020) 148.
- [44] T. G. Khunjua, K. G. Klimenko, and R. N. Zhokhov, Influence of chiral chemical potential μ_5 on phase structure of the two-color quark matter, *Phys. Rev. D* **106**, 045008 (2022).
- [45] Nils Strodthoff, Bernd-Jochen Schaefer, and Lorenz von Smekal, Quark-meson-diquark model for two-color QCD, *Phys. Rev. D* **85**, 074007 (2012).
- [46] Nils Strodthoff and Lorenz von Smekal, Polyakov-quark-meson-diquark model for two-color QCD, *Phys. Lett. B* **731**, 350 (2014).
- [47] Naseemuddin Khan, Jan M. Pawłowski, Fabian Rennecke, and Michael M. Scherer, The phase diagram of QC2D from functional methods, [arXiv:1512.03673](https://arxiv.org/abs/1512.03673).

- [48] Romain Contant and Markus Q. Huber, Dense two-color QCD from Dyson-Schwinger equations, *Phys. Rev. D* **101**, 014016 (2020).
- [49] Daiki Suenaga and Toru Kojo, Gluon propagator in two-color dense QCD: Massive Yang-Mills approach at one-loop, *Phys. Rev. D* **100**, 076017 (2019).
- [50] Toru Kojo and Daiki Suenaga, Thermal quarks and gluon propagators in two-color dense QCD, *Phys. Rev. D* **103**, 094008 (2021).
- [51] Daiki Suenaga and Toru Kojo, Delineating chiral separation effect in two-color dense QCD, *Phys. Rev. D* **104**, 034038 (2021).
- [52] Toru Kojo and Daiki Suenaga, Peaks of sound velocity in two color dense QCD: Quark saturation effects and semi-short range correlations, *Phys. Rev. D* **105**, 076001 (2022).
- [53] Toru Kojo and Daiki Suenaga, Meson resonance gas in a relativistic quark model: Scalar vs vector confinement and semishort range correlations, [arXiv:2208.13312](https://arxiv.org/abs/2208.13312).
- [54] Gordon Baym, Tetsuo Hatsuda, Toru Kojo, Philip D. Powell, Yifan Song, and Tatsuyuki Takatsuka, From hadrons to quarks in neutron stars: A review, *Rep. Prog. Phys.* **81**, 056902 (2018).
- [55] Kotaro Murakami, Daiki Suenaga, Etsuko Itou, and Kei Iida (to be published).
- [56] Murray Gell-Mann and M Levy, The axial vector current in beta decay, *Nuovo Cimento* **16**, 705 (1960).
- [57] Tetsuo Hatsuda and Teiji Kunihiro, QCD phenomenology based on a chiral effective Lagrangian, *Phys. Rep.* **247**, 221 (1994).
- [58] Bernd-Jochen Schaefer and Jochen Wambach, Susceptibilities near the QCD (tri)critical point, *Phys. Rev. D* **75**, 085015 (2007).
- [59] Vivek Kumar Tiwari, Exploring criticality in the QCD-like two quark flavour models, *Phys. Rev. D* **86**, 094032 (2012).
- [60] Tina K. Herbst, Jan M. Pawłowski, and Bernd-Jochen Schaefer, Phase structure and thermodynamics of QCD, *Phys. Rev. D* **88**, 014007 (2013).
- [61] Shuntaro Sakai and Daisuke Jido, In-medium η' mass and η'/N interaction based on chiral effective theory, *Phys. Rev. C* **88**, 064906 (2013).
- [62] Abdel Nasser Tawfik and Abdel Magied Diab, Polyakov SU (3) extended linear- σ model: Sixteen mesonic states in chiral phase structure, *Phys. Rev. C* **91**, 015204 (2015).
- [63] Abdel Nasser Tawfik and Niseem Magdy, SU(3) polyakov linear- σ model in magnetic fields: Thermodynamics, higher-order moments, chiral phase structure, and meson masses, *Phys. Rev. C* **91**, 015206 (2015).
- [64] G. Fejős and A. Hosaka, Mesonic and nucleon fluctuation effects at finite baryon density, *Phys. Rev. D* **95**, 116011 (2017).
- [65] G. Fejos and A. Hosaka, Axial anomaly and hadronic properties in a nuclear medium, *Phys. Rev. D* **98**, 036009 (2018).
- [66] Daiki Suenaga and Phillip Lakaschus, Comprehensive study of mass modifications of light mesons in nuclear matter in the three-flavor extended linear σ model, *Phys. Rev. C* **101**, 035209 (2020).
- [67] Abdel Nasser Tawfik, Abdel Magied Diab, and M. T. Hussein, Chiral phase structure of the sixteen meson states in the SU(3) polyakov linear-sigma model for finite temperature and chemical potential in a strong magnetic field, *Chin. Phys. C* **43**, 034103 (2019).
- [68] Hong Mao, Nicholas Petropoulos, and Wei-Qin Zhao, The linear sigma model at a finite isospin chemical potential, *J. Phys. G* **32**, 2187 (2006).
- [69] Andrei V. Smilga and J. J. M. Verbaarschot, Spectral sum rules and finite volume partition function in gauge theories with real and pseudoreal fermions, *Phys. Rev. D* **51**, 829 (1995).
- [70] K. Splittorff, D. T. Son, and Misha A. Stephanov, QCD—Like theories at finite baryon and isospin density, *Phys. Rev. D* **64**, 016003 (2001).
- [71] Jonathan T. Lenaghan, Dirk H. Rischke, and Jurgen Schaffner-Bielich, Chiral symmetry restoration at nonzero temperature in the $SU(3)_r \times SU(3)_l$ linear sigma model, *Phys. Rev. D* **62**, 085008 (2000).
- [72] Bernd-Jochen Schaefer and Mathias Wagner, The three-flavor chiral phase structure in hot and dense QCD matter, *Phys. Rev. D* **79**, 014018 (2009).
- [73] Denis Parganlija, Peter Kovacs, Gyorgy Wolf, Francesco Giacosa, and Dirk H. Rischke, Meson vacuum phenomenology in a three-flavor linear sigma model with (axial-) vector mesons, *Phys. Rev. D* **87**, 014011 (2013).
- [74] M. Kobayashi and T. Maskawa, Chiral symmetry and $\eta - X$ mixing, *Prog. Theor. Phys.* **44**, 1422 (1970).
- [75] M. Kobayashi, H. Kondo, and T. Maskawa, Symmetry breaking of the chiral $U(3) \otimes U(3)$ and the quark model, *Prog. Theor. Phys.* **45**, 1955 (1971).
- [76] Gerard 't Hooft, Computation of the quantum effects due to a four-dimensional pseudoparticle, *Phys. Rev. D* **14**, 3432 (1976); **18**, 2199(E) (1978).
- [77] Gerard 't Hooft, Symmetry Breaking Through Bell-Jackiw Anomalies, *Phys. Rev. Lett.* **37**, 8 (1976).
- [78] Edward Witten, Baryons in the $1/n$ expansion, *Nucl. Phys. B* **160**, 57 (1979).
- [79] P. Di Vecchia and G. Veneziano, Chiral dynamics in the large N limit, *Nucl. Phys. B* **171**, 253 (1980).
- [80] K. Splittorff, D. Toublan, and J. J. M. Verbaarschot, Diquark condensate in QCD with two colors at next-to-leading order, *Nucl. Phys. B* **620**, 290 (2002).
- [81] Kotaro Murakami, Daiki Suenaga, Kei Iida, and Etsuko Itou, Measurement of hadron masses in 2-color finite density QCD, *Proc. Sci. LATTICE2022* (2023) 154 [[arXiv:2211.13472](https://arxiv.org/abs/2211.13472)].
- [82] G. Fejos and A. Hosaka, Thermal properties and evolution of the $U_A(1)$ factor for $2 + 1$ flavors, *Phys. Rev. D* **94**, 036005 (2016).
- [83] R. L. Workman, *et al.* (Particle Data Group), Review of particle physics, *Prog. Theor. Exp. Phys.* **2022**, 083C01 (2022).
- [84] Yohei Kawakami and Masayasu Harada, Analysis of $\Lambda_c(2595)$, $\Lambda_c(2625)$, $\Lambda_b(5912)$, $\Lambda_b(5920)$ based on a chiral partner structure, *Phys. Rev. D* **97**, 114024 (2018).
- [85] Yohei Kawakami and Masayasu Harada, Singly heavy baryons with chiral partner structure in a three-flavor chiral model, *Phys. Rev. D* **99**, 094016 (2019).
- [86] Masayasu Harada, Yan-Rui Liu, Makoto Oka, and Kei Suzuki, Chiral effective theory of diquarks and the $U_A(1)$ anomaly, *Phys. Rev. D* **101**, 054038 (2020).

- [87] Yonghee Kim, Emiko Hiyama, Makoto Oka, and Kei Suzuki, Spectrum of singly heavy baryons from a chiral effective theory of diquarks, [Phys. Rev. D **102**, 014004 \(2020\)](#).
- [88] Yohei Kawakami, Masayasu Harada, Makoto Oka, and Kei Suzuki, Suppression of decay widths in singly heavy baryons induced by the $U_A(1)$ anomaly, [Phys. Rev. D **102**, 114004 \(2020\)](#).
- [89] Daiki Suenaga and Atsushi Hosaka, Novel pentaquark picture for singly heavy baryons from chiral symmetry, [Phys. Rev. D **104**, 034009 \(2021\)](#).
- [90] Daiki Suenaga and Atsushi Hosaka, Decays of roper-like singly heavy baryons in a chiral model, [Phys. Rev. D **105**, 074036 \(2022\)](#).